Proceedings of the ASME 2010 3rd Joint US-European Fluids Engineering Summer Meeting and 8th International Conference on Nanochannels, Microchannels, and Minichannels
FEDSM-ICNMM2010
August 1-5, 2010, Montreal, Canada

FEDSM-ICNMM2010-30738

CHARACTERIZATION OF THE RESPONSE OF A CURVED ELASTIC SHELL TO TURBULENT BOUNDARY LAYER

Francesca Magionesi
INSEAN
Rome, Italy

Elena Ciappi
INSEAN
Rome, Italy

ABSTRACT
For the effective operation of sonar system mounted inside the bulbous of a fast ship, it is important to reduce all the possible noise and vibration sources that cause the dome to vibrate thus radiating noise and interfering with sonar sensor response. In particular, pressure fluctuations induced by the turbulent boundary layer on the surface of the sonar dome represent one of the major sources of self-noise for the on board sensors. Calculation of the structural vibrations and of the noise radiated inside the dome requires as a first step the characterization of the frequency spectra of turbulent boundary layer excitation. Most of the literature related to wall pressure fluctuations is devoted to the study of equilibrium turbulent boundary layers on flat plates in zero pressure gradient (ZPG) flow, for which scaling laws for the power spectral densities and empirical models for the cross spectral densities are well established. The turbulent boundary layer on the bulbous can present several differences with respect to the canonical case because of the presence of hull surface curvatures and of the free water surface that produce pressure gradient variation along the bulbous surface. Moreover, hydrodynamic coincidence effects play a markedly different role in the underwater problem than in the aerodynamic problem. Therefore, an experimental campaign was performed in a towing tank to measure wall pressure fluctuations at different locations along a large scale model of a bulbous and to investigate their spectral characteristics in terms of auto and cross spectral densities. Boundary layer mean flow parameters were obtained with a finite volume code solving the Reynolds Averaged Navier Stokes Equations. The auto spectral densities (ASD) of the measured wall pressure fluctuations were scaled using different combinations of inner and outer flow parameters in order to make ASD independent of the tested conditions *i.e.* of Reynolds number. The modelled load was used as input for a numerical procedure aimed at evaluating the dynamical response of a section of the bulbous under analysis. The validation of this procedure was experimentally obtained through the measurements of the vibrational response of an elastic section inserted into the bulbous model. Moreover, this comparison indirectly provides additional insights on the physics of wall pressure fluctuations for complex flows.

INTRODUCTION.
Vibrations induced by turbulent boundary layer excitation acting along the bulbous of a fast ship can be potentially responsible for degradation in the functioning of sonar system. The characterization of the dynamical behaviour of elastic structures subjected to TBL load is a very complex and changeling interdisciplinary argument, which involves a deep knowledge of both fluid dynamic and structural dynamic.
Despite in the last 40 years wall pressure fluctuations induced by turbulent boundary layer (TBL) has received great attention by the research community, the majority of technical publications on this subject concern only simplified geometries (flat plate and cylinder) and ideal flow conditions (equilibrium boundary layer with zero pressure gradient) [1, 2].
The TBL on a more complex geometry, such as the bulbous of a ship, can present several differences with respect to the canonical case, because of the presence of surface curvatures and of the free water surface that produce pressure gradient variation along the bulbous surface. Moreover, when a body moves through a fluid the boundary layer on its surface becomes turbulent only after the development of a transitional region from the laminar state characterized by strong instability and pressure fluctuations on the body surface. The characterization of pressure loads induced by transition from laminar to turbulent is still an open problem. Recently, in reference 3 the authors have provided an interesting attempt to model the space time characteristics of wall pressure

fluctuations in the wavenumber frequency spectrum under transitional boundary layer. Their model assumes that this last is the convolution of the spectrum of a fully developed turbulent boundary layer, modelled using Corcos expression[4], with that of the intermittency function, which provides the number of turbulent spots acting in the transition region experimentally evaluated. As to the authors known, no publications directly analyses the vibration induced on an elastic structure to this load.

The evaluation of the response of elastic structures under TBL load requires as a first step the characterization of the frequency spectra of TBL excitation acting on it. Wall pressure fluctuations induced by TBL excitation is a stochastic process and its cross spectral density (CSD) is usually the quantity used for its complete representation. It can be expressed as a product of the auto power spectrum (ASD) in a reference point and a spatial correlation function. Wall pressure spectra for equilibrium flows have been extensively studied and a review of the literature is provided in Ref.1. Several studies have addressed the issue of scaling wall pressure spectra in order to make ASD independent of the tested conditions *i.e.* of Reynolds number[5-8]. It is not possible to find a unique scaling law that leads to the collapse of various regions of wall pressure spectra in all the frequency range, since different frequency ranges of pressure spectra correspond to contributions from velocity fluctuations in different region of the boundary layer.

However, in technical literature different combinations of inner and outer flow parameters have been proposed for the collapse of pressure spectra in different frequency ranges.

Recently, Goody[9] has proposed a semi-empirical model for the pressure ASD valid for a 2D zero pressure gradient boundary layer, which includes Reynolds number effect, that seems to provide a good representation of the pressure load.

The presence of pressure gradients and curvatures implies a reanalysis of the more suitable scaling parameters that produce spectra collapse. Previous works addressing the effects of curvature and pressure gradients were basically conducted on specially design setup and simplified models where those effects are suitable divided. In particular, Schlomer[10] analysed the different effects produced by adverse and favourable pressure gradients on the development of boundary layer. In particular, an adverse pressure gradient (APG), that usually develops in the first part of a ship bulbous, is responsible of a reduction of the convection velocity of turbulent eddies along the boundary and an increase of the root mean square of pressure, due to the higher contribution of the low- and mid-frequency ranges while no significant changes in pressure spectra arises at high frequency. On the contrary, a favourable pressure gradient (FPG) produces higher amplitude in the low frequency part but a strong decrease in the high frequency region. These results were partially confirmed by the numerical simulations of Na and Moin[7].

Gillis and Johnston[11] analyzed TBL acting on a convex wall separating the effects induced by the presence of pressure longitudinal gradient, which was forced to be zero over the test section. They observed that unlike the flat plate case, the radius of curvature rather than the boundary layer thickness should be used for the scaling of velocity profile. The effects of transverse curvature begins to alter the characteristics of the flow only for $\delta/R > O(1)$ where δ is the boundary layer thickness and R the radius of curvature, causing a variation of the slope of the logarithmic region and an increase in the friction velocity in comparison to flat plate flows at comparable Reynolds numbers. These aspects have obviously a direct consequence in the wall pressure spectra, giving rise to a shift of energy from the low to high frequency[2].

On the contrary, it is quite unclear whether pressure gradients and wall curvature interacts.

The second element necessary for the modelling of wall pressure induced by equilibrium boundary layer is the spatial correlation function. A number of models have been proposed for the prediction of the fluctuating pressure field for equilibrium boundary layer[4,12-14].

The first model was developed by Corcos[4], who proposed a wavenumber frequency spectrum for the cross spectral density which is dominated by the convective terms. Despite this hypothesis it can be consider a good approximation in a number of applications, *i.e.* for structures where the bending wavenumebers k_B are close to the convective ones $k_c = \omega/U_c$. In the naval field, characterized typically by structural wavenumbers lower than k_c, this model can overpredicts the response in the subconvective region[15,16]. Based on these results, Chase[12] extended the model including the low wavenumber contributions of the spectra. These improvements on the CSD model have as a counterpart an increase of complexity in the model parameter identifications (that also seems quite sensitive to experimental conditions) and in the implementation on structural code for the identification of the dynamical response of structure to TBL load.

On the contrary, the success of Corcos model relies on its simplicity and on its predictive character since the model parameters are substantially case independent.

These existing models for CSD of the fluctuating pressure are based on fits to data under ideal conditions and can be deficient when applied to real structures. Despite real conditions may greatly differ from those, only few works concern the effect of pressure gradients and wall curvature on the applicability of classical CSD model[10].

An indirect verification of the goodness of the CSD model used for the characterization of the wall pressure fluctuation can be obtained by comparing the measured response of an elastic structure subjected to this load with that predicted numerically using the wall pressure models.

The first attempt to make a direct comparison of measured and predicted vibration induced by TBL was made by Finnveden et al.[16] for a flat plate in a wind tunnel and by Ciappi et al.[15] on a plate inserted into the hull bottom of a catamaran in a towing tank. For both cases the considered structures are simple plates and TBLs are supposed to be fully developed.

The results presented in Ciappi et al[15] are here generalized by analysing a curved elastic shell inserted into the bulbous of a fast ship. The applicability of Corcos model for CSD will be verified analysing both wall pressure fluctuation measurements performed along the bulbous and the dynamic response of an elastic shell inserted into the bulbous. Moreover, interesting insights into the transition region are given by analysing lower velocity spectra, when transition acts, and the related structural response.

Using the modelled load an in-house program was developed to evaluate the response of the aforementioned structure to the random pressure field generated by the boundary layer.

In the developed method a weak coupling between the structure and the fluid is assumed *i.e.* in the modelling of the load the structure is supposed rigid but the effect of the fluid is taken into account when evaluating the structural modal parameters.

NOMENCLATURE

d pressure sensor diameter

d^+ d normalized by the viscous length scale $d\,u_\tau/\nu$

Fr Froude number $U/g\,L$

H structural transfer function matrix

L length of the bulbous

Re_θ Reynolds number based on momentum thickness $U\,\theta/\nu$

U free stream velocity

U_c wall pressure convection velocity

u_τ friction velocity

S_w matrix of the CSD of the plate displacement

S_Φ matrix of the CSD of the generalised load

S_{FF} matrix of the CSD of the equivalent load

β Clauser parameter $\dfrac{\delta^*}{\tau_W}\dfrac{dp}{dx}$

γ_1, γ_2 stream-wise and span-wise decay factors

Γ coherence function

δ boundary layer thickness

δ^* boundary layer displacement thickness

θ boundary layer momentum thickness

ϑ phase of cross spectral density of pressure signals

η sensor spanwise separation

ν kinematic viscosity

ξ sensors streamwise separation

τ_w wall shear stress

ϕ_{pp} wall pressure autospectrum

$\phi_{pp'}$ wall pressure cross spectrum

Φ matrix of eigenvectors

ω radian frequency

ω_i i-th natural frequency of the shell

TEST FACILITY AND TEST MODEL

The experimental campaign was performed in the Insean towing tank n°1, which is 470 m long, 13.5 m wide and 6.5 m deep. The object of study is a 1:8 scale model of a bulbous of a fast ship (see fig. 1). The analysed section is located 70 cm from the stagnation point, corresponding to a value of $x/L = 0.2$ (fig. 4), in a region of mild longitudinal and transversal curvatures.

Behind the bulb a suitable geometry has been designed to prevent hydrodynamic disturbances. Preliminary numerical simulations of the flow around the structure permitted to verify the absence of strong wave breaking phenomena close to the measuring region that can mask the pressure fluctuations due to TBL.

The model is 4.63 m long, of which only the first 2.294 m belongs to the bulbous geometry, and the draft is above 1 m. The model was rigidly connected to the carriage over the tank as shown in figure 1.

Figure 1 Experimental setup

NUMERICAL SIMULATION

A proper calculation of flow noise caused by boundary layer pressure fluctuations requires knowledge of flow parameters. Since direct measurements of boundary layer parameters required long and difficult velocity measurements, numerical simulations of the flow around the bulbous were carried out to evaluate the mean flow data, necessary to derive suitable scaling parameters for ASD pressure collapse. A finite volume code solving the Reynolds Averaged Navier Stokes Equations that use a Level Set technique to capture the free surface was used. The details of the RANS code used for the numerical simulation can be obtained in Ref.17. The results of these simulations in terms of mean flow data are summarized in table 1. In figure 2 the pressure coefficients distribution $c_p = \left(p - p_{ref}\right) \Big/ \left(\frac{1}{2}\rho U^2\right)$ evolving along the bulbous for the different velocities are depicted. The variation of pressure gradient along the bulbous implies that the flow is not selfsimilar. In literature[7] the Clauser's equilibrium parameter $\beta = \frac{\delta^*}{\tau_W} \frac{dp}{dx}$ is usually used for the characterization of the pressure gradient magnitude. The values assumed by β for the different Froude number are summarized in table 1.

Table 1: mean flow data

U(m/s)	Fr	δ	δ^*	Re_θ	u_τ	τ_w	β
6.36	1.34	5.6e-3	8.27e-4	3248	0.277	76.73	0.093
5.45	1.15	5.7e-3	8.52e-4	2841	0.239	57.12	0.095
3.64	0.76	6.0e-3	9.3 e-4	2033	0.164	26.89	0.096
2.72	0.57	6.3e-3	9.80e-4	1580	0.126	15.87	0.085

It is evident a presence of a mild adverse pressure gradients for all the tested conditions.

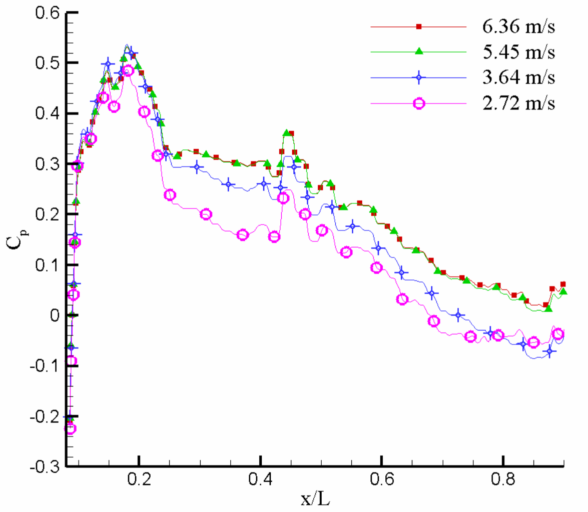

Figure 2 Pressure coefficient distribution

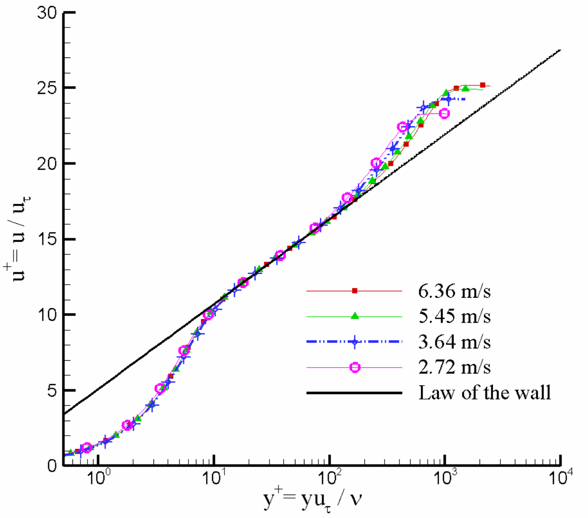

Figure 3 Velocity profiles - law of the wall

This consideration is confirmed from the analysis of the velocity profiles (see fig. 3), in fact it is evident a reduction of the region of validity of the law of the wall $\left(20 < y^+ < 200\right)$ with respect the value typical of ZPG. Thus, the combined effects of curvature and streamwise pressure gradient are more evident in the outer region. On the other hand, inner variables adequately account for these effects in the near wall and logarithmic regions.

PRESSURE MEASUREMENTS

The first experimental campaign has been devoted to measure wall pressure fluctuations induced by the boundary layer attached along the model. The measurements of pressure fluctuations along the bulbous have been accomplished with an array of piezoelectric transducers KULITE XCL-072, characterized by a sensitivity of 20 mV/psi, a resonant frequency of 100 kHz and an external diameter equal to 1.8 mm, corresponding to values of the nondimensional parameter $d^+ = d\,u_\tau / \nu$ varied between $174 \div 383$ depending on the free stream velocity. The array consisted of 8 pressure transducers, of which 5 were flush mounted with the bulbous surface in streamwise direction and other 3 transducers in the transversal direction, as shown in figure 5. The small dimension of the probe has allowed reducing the surface discontinuity with the model external surface.

Figure 4 1:8 model scale

Figure 5 Measuring section

Data were recorded using LMS scadas Mobile acquisition system. The frequency is sampled at 25000 Hz. The acquisition time is 20 seconds for the higher velocity runs and 30 seconds for the lower ones. Moreover the signals of three accelerometers, which were mounted inside the bulbous close to the pressure transducers and in the connecting frame between the model and the carriage, were recorded to identify the structural vibrations transmitted from the structure to the model affecting the PSD of pressure signals in the very low frequency region.

Statistic features of pressure fluctuations

Before discussing the applicability of the scaling laws for the single point pressure spectra it is fruitful to make some preliminary considerations on the dimensional ones. In figure 6 the ASD of pressure fluctuations for the four velocity conditions are depicted. It is evident a different behaviour between the curves relative to higher velocities (corresponding to 6.36 and 5.45 m/s) and those relative to 3.64 and 2.72 m/s. In particular, the higher velocities spectra are typical of a fully developed TBL with the characteristic smooth and quite flat trend at low frequencies. On the contrary, at 3.64 m/s pressure spectrum is characterised by a broad hump typical of late transitional phenomena, due to Tollmien-Schlichting waves[18]. Finally, at the lowest tested velocity the pressure spectrum has a totally different behaviour: the typical flat and smooth spectrum related to a TBL is modified in a spectrum characterized by strong amplitude oscillations. As it can be seen in table 1 local Reynolds number is really low for this velocity, thus pressure transducers are certainly located in a region of transition between laminar to turbulent boundary layer. In this case the energy content is sensibly lower than for the other spectra.

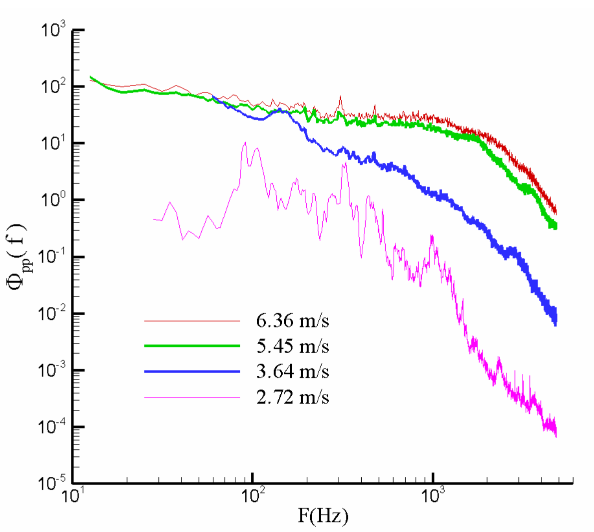

Figure 6 Dimensional ASD

There is no unique scaling law that collapse the pressure spectra with different Reynolds numbers at all frequency. Traditionally, two scaling laws were applied to collapse the pressure spectrum in specific frequency ranges. The high frequency spectrum collapse well when normalized using inner flow variable: $u_\tau^2/\left(\nu\,\tau_w^2\right)$ as pressure scale and ν/u_τ^2 as time-scale. In the low- and middle-frequency ranges the same agreement on the definition of pressure and time scale is not verified. For these frequency ranges, a good choice for the collapse of pressure data is: δ/u_τ for the frequency axis and $u_\tau/\left(\delta\,\tau_w^2\right)$ for pressure amplitude.

Moreover, the presence of curvature and of pressure gradients highly complicates these analyses.

In figures 7 and 8 the dimensionless wall pressure spectra are depicted using inner and outer flow variables, respectively and compared with experimental results performed with flat plates in ZPG flow conditions[5,19,20].

From the analysis of figure 7 it is evident that, except for the lower velocity, at high frequency a good collapse of pressure data when using inner flow variables arises. Moreover, as several investigation have shown[11,21], a logarithmic region can be still observed in flow with longitudinal curvature and pressure gradients, although the flat plate constant of the log law can be modified.

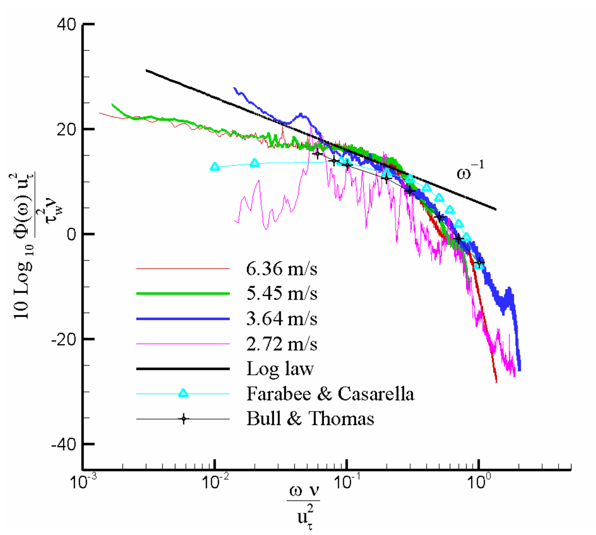

Figure 7 ASD scaled using inner variables

On the contrary, the use of flow parameters that belong to the outer flow region (Fig. 8) do not provide a good collapse of data for all the tested velocities.

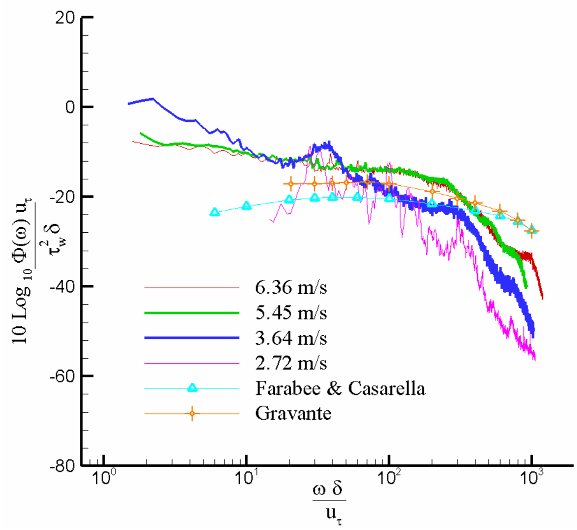

Figure 8 ASD scaled using outer variables

Moreover, compared with equilibrium flow with zero pressure gradient measured by Farabee[5] and Gravante[20], the measured spectrum levels are higher in the lower frequency range. This behaviour also underlined by Schloemer[10] is related to an increase of the longitudinal turbulence intensity over the inner two-third of the boundary layer. As discussed above, at 3.64 m/s (corresponding to Froude number 0.76) there is evidence of a broad hump in the pressure spectrum for $\omega\delta^* / U = 0.2$. This broad hump has been already underlined in pressure spectra at low Reynolds number at the same value of dimensionless frequency[18]. Again pressure spectrum relative to 2.62 m/s does not collapse even if a logarithmic slope is still visible at least in a tangential sense.

In a classical wall pressure fluctuations data analysis, once the ASD of the pressure fluctuations is correctly scaled, a spatial correlation function must be evaluated for the complete representation of the turbulent load. This information can be obtained from the analysis of the coherence functions among the sensors.

The base of this work is the Corcos model of cross spectral density[4]. From previous analyses[22] Corcos postulated that CSD of pressure signals depends only on the similarity variables $\frac{\omega\xi}{U_c}$ and $\frac{\omega\eta}{U_c}$, where ξ, η are the spatial separations in streamwise and spanwise directions and U_c is the convection velocity. The Corcos expression for the coherence function between two pressure signals is expressed by:

$$\Gamma(\omega,\xi,\eta) = e^{-\gamma_1 \frac{\omega\xi}{U_c}} e^{-\gamma_2 \frac{\omega\eta}{U_c}} \qquad (1)$$

where γ_1 and γ_2 are two factors that represent the rate of decay of the turbulent eddies, *i.e.* the loss of coherence, to be evaluated by fitting the exponential curve with the experimental results. In fact, it is well known that they are dependent on the presence of pressure gradients and also slightly on the Reynolds number.

In the CSD model convection velocity is usually considered a constant fraction of the free stream velocity varying between 0.6 in presence of high APG and 0.8 for the ZPG case. While this approximation is usually sufficient for the correct modeling of the TBL load, it is important to underline that the real trend is more complex. Starting from the phase of the streamwise cross-spectral density ϑ, the convection velocity can be determined as $U_C = -\omega\xi/\vartheta$. In figure 9 convection velocities at 5.45 m/s as a function of frequency for two different spatial separations are plotted.

It is evident that as far as the longitudinal spacing is incremented, the convection velocity increases. This is due to the fact that the group of eddies traveling along the surface are convected along the boundary layer with different velocities and have different "life time". In fact, while small scale eddies are slower and rapidly destroyed, the large scale eddies traveling at higher velocities dominate when spatial separation increases implying an increase of U_c. The same results were obtained for the other tested velocities, except for the 15 knots where the fluctuations of pressure spectra, especially in the low frequency range, due to transitional effects, mask totally the convection velocity behavior.

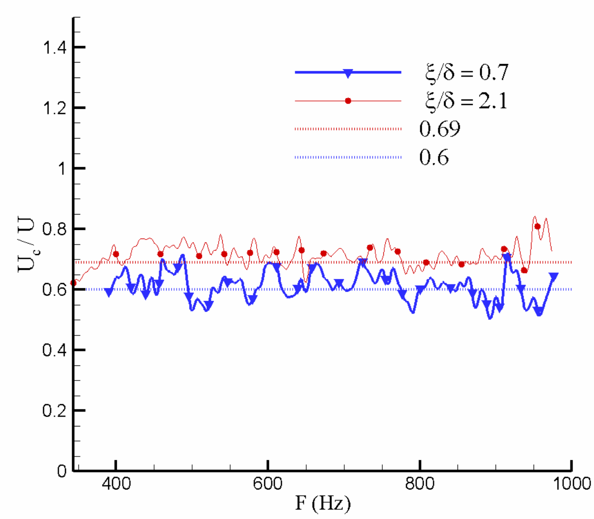

Figure 9 Convection velocity at 5.45 m/s

Convection velocity can be also obtained as the ratio ξ/τ at which the cross-correlation $R_{pp}(\xi,\tau)$ reaches a maximum. In figure 10 the broadband convection velocity at 5.45 m/s obtained from the analysis of the space-time correlation function of pressure signals is depicted.

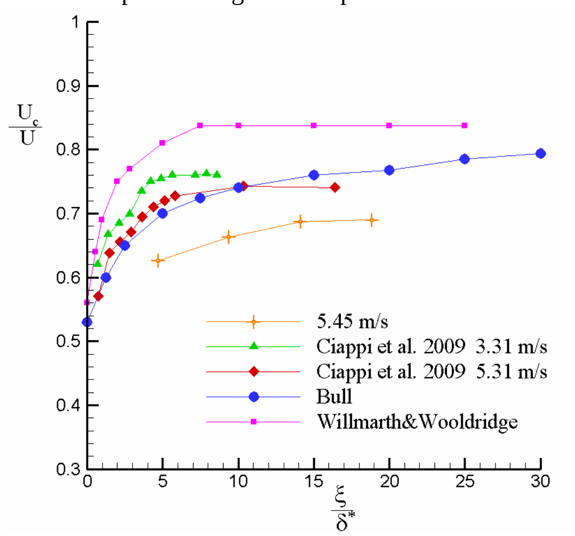

Figure 10 Broad band convection velocity

The present result normalized with respect to the free stream velocity as a function of the dimensionless parameter ξ/δ^* is compared with those obtained experimentally by Bull[1], Willmarth et al.[22] and Ciappi et al.[15]. The value of U_c ranges from 0.6 for the smaller separations, associated with the small-scale structures, to 0.69 at higher separations, related to the larger scale structures. The lower asymptotic value assumed by U_c agree qualitatively well with the results of Schloemer for mild APG. Thus, as proposed by several author, U_c can be modelled with a constant average value, in this case equal to 0.65*U*.

In figure 11 the streamwise coherence is plotted as a function of dimensionless frequency $\frac{\omega\xi}{U_c}$ for different spatial separations and compared with Corcos expression. Compared with classical value obtained by Corcos (i.e. $\gamma_1 = 0.125$) for fully developed TBL over a flat plate, the actual streamwise coherence has a faster decay $\gamma_1 = 0.19$. This increment is in agreement with the results of Schlomer for mild adverse pressure gradient. On the contrary, from the analysis of the spanwise coherence it was not possible to identify exactly the decay rate. In fact, even at the smallest spanwise spatial separation $(\eta/\delta = 0.66)$, the coherence assumes value too low to be distinguished from the background noise. Since previous studies[2,10] have demonstrated that spanwise coherence are less dependent on pressure gradient than that measured in the streamline direction, classical Corcos decay factor will be used to model γ_2 in the evaluation of structural response in the following section, thus $\gamma_2 = 0.7$.

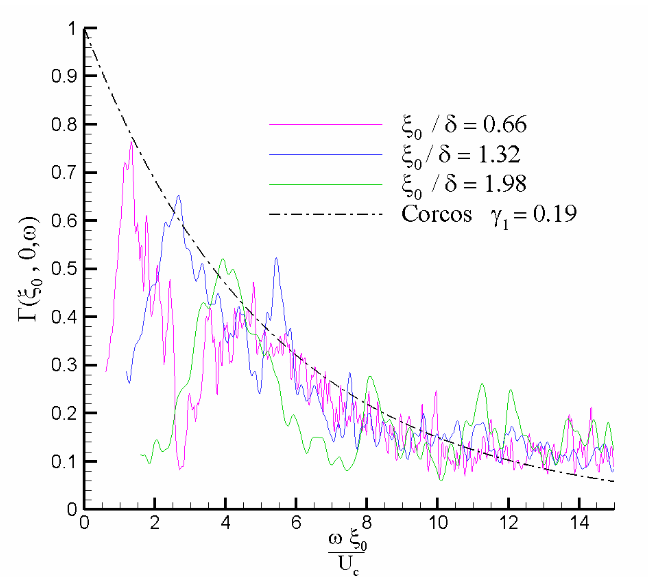

Figure 11 Streamwise coherence at 20 knots

Concerning pressure measurements performed at 15 knots, it is interesting to underline a totally different behavior. In fact for both stream- and spanwise- spatial separations, due to the presence of strong oscillations, pressure signals remain highly correlated for a wide frequency range.

ACCELERATION MEASUREMENTS

The dynamical response of the section of the bulbous to turbulent boundary layer excitation was experimentally evaluated. The section under analysis is a double curved rectangular Plexiglas shell 4 mm thick (see fig. 12). Its dimensions calculated as a projection of its surface on a plane are 25 x 20 cm.

The dynamical response of the structure was measured using 12 accelerometers (PCB 333B32), characterized by a sensitivity of 10.19 mV/(m/s^2) and a weight of 4 gr. Due to the considerable weight of the sensors with respect to that of the shell, the dynamic response of the plate in dry conditions results significantly varied. However, when the bulbous is covered by the water, the effects of the accelerometer masses are less important because of the contribution of the added mass due to water loading which highly increment the mass of the coupled system (shell and water). Time signals were acquired using 40 channel LMS SCADAS Mobile acquisition system, the sample rate is the same used for pressure measurements.


Figure 12 Vibration measurements set up

Preliminary *in vacuo* and *coupled* modal analysis was performed using hammer impact test. As expected, the presence of water on one side of the shell highly changes its natural frequencies causing a strong reduction of their first orders values. The first seven identified natural frequencies are reported in table 2.

Table 2: identified natural frequency

Dry natural frequency	Wet natural frequency
865	223
613	240
805	288
864	339
920	356
1069	415
1105	431

Hammer impact test allowed at determining also the modal damping in dry and wet conditions equal to 0.028 and 0.054, respectively.
Acceleration acquisitions were performed at the same velocities analysed for the pressure measurements.

COMPUTATIONAL METHOD

The results presented in Ciappi et al[15] are here generalized by analysing the curved elastic shell inserted into the bulbous.

The numerical approach used to obtain the structural response of a section of bulbous excited by turbulent boundary layer is here briefly summarized. The dynamical response of a discretized structure subjected to a generic stochastic distributed load can be expressed in terms of cross spectral density matrix of displacement $S_w(\omega)$ as follows[23]:

$$S_w(\omega) = \Phi\, H(\omega) S_\Phi(\omega) H(\omega)^* \,\Phi^T \qquad (2)$$

where Φ is the matrix of modes of the structure, $H(\omega)$ is the transfer function matrix which element is $H_j(\omega) = \left[\omega_j^2 - \omega^2 + i\eta\omega_j^2\right]^{-1}$ and $S_\Phi(\omega)$ is the matrix of the generalized forces, which can be evaluated from:

$$\left[S_\Phi(\omega)\right] = [\Phi]^T \left[S_{FF}(\omega)\right] [\Phi] \qquad (3)$$

The shell is divided into small finite elements, each of which is approximated to a flat plate.

The continuous random wall pressure field is approximated using a finite set of discrete forces acting on the nodal points using the following expression:

$$\mathbf{S}C^{(G)}_{FF\ i,j} = \int_{x_i-\frac{\Delta x}{2}}^{x_i+\frac{\Delta x}{2}} \int_{x_j-\frac{\Delta x}{2}}^{x_j+\frac{\Delta x}{2}} \int_{y_i-\frac{\Delta y}{2}}^{y_i+\frac{\Delta y}{2}} \int_{y_j-\frac{\Delta y}{2}}^{y_j+\frac{\Delta y}{2}} \Phi_{pp'}(x_i, x_j, y_i, y_j, \omega)\, dy_j\, dy_i\, dx_j\, dx_i \qquad (4)$$

where $\mathbf{S}C^{(G)}_{FF\ i,j}$ is the generic i,j element of the load matrix, $\Delta x \Delta y$ is the area assigned to the points $P_1(x_r, y_r)$ and $P_2(x_s, y_s)$. Thus the load acting on each point of the grid is the results of the distributed load acting on the equivalent nodal area, which is evaluated using a deterministic pressure load of unit amplitude as shown by De Rosa et al.[24] .
In eq (4) the pressure load is expressed using Corcos model with the identified parameters and pressure measured spectra.

Numerical simulations were performed for all the tested velocities in a frequency range between 200 and 1500 Hz with a frequency step of 1 Hz. For a correct estimation of the structural behavior 50 modes were used. They were evaluated using a commercial finite element code COMSOL, taking into account the effects of fluid loading.

VERIFICATION OF THE METHOD

In this paragraph the comparison of the numerical and the experimental response of the elastic shell are presented. Both numerical and experimental responses were spatially averaged over the 12 measurement points.

In figure 13 the experimental responses for all the velocities are depicted. It is interesting to notice that despite pressure measurements at 2.62 m/s are between 2 and 3 orders of magnitude lower than those measured for the other velocities, the dynamical response to this load is comparable with the 3.64 m/s case in particular in the mid and high frequency ranges. This experimental evidence suggests that transition may be more effective than a fully developed TBL in forcing structural vibrations as already underlined in Ref.3. The results at the highest velocity (*i.e.* 6.36 m/s) show that even if no significant changes in the response trend with respect to the 5.45 m/s case can be observed, the dynamical behaviour of the shell is covered by disturbances due to an increase of the carriage vibrations and to strong wave breaking phenomena close to the measurement section. For this reason the comparison with numerical simulations at 6.36 m/s will be not discussed.

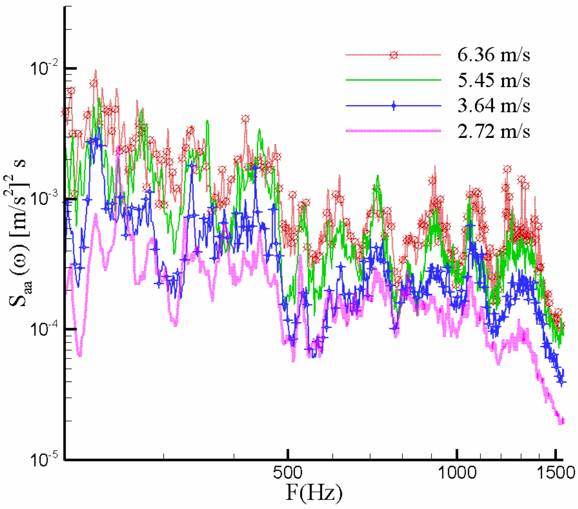

Figure 13 Experimental ASD of the shell acceleration

In figures 14-16 the comparisons between the numerical and the experimental dynamical response of the shell for 5.45, 3.64 and 2.72 m/s are shown, respectively.

In the low-mid frequency ranges the agreement for 5.45and 3.64 m/s is good. At higher frequency, while for 30 knots the agreement is still good (even as expected an overestimate of Corcos model arises), at 3.64 m/s the numerical procedure lightly underestimates the accelerometer results. It is important to notice that despite some transitional phenomena still arises at this last velocity, as underlined analysing pressure signals, the quite good agreement with the numerical result obtained under the hypothesis of fully developed turbulent boundary layer, implies that no significant changes in the pressure model of CSD of wall pressure fluctuations is necessary.

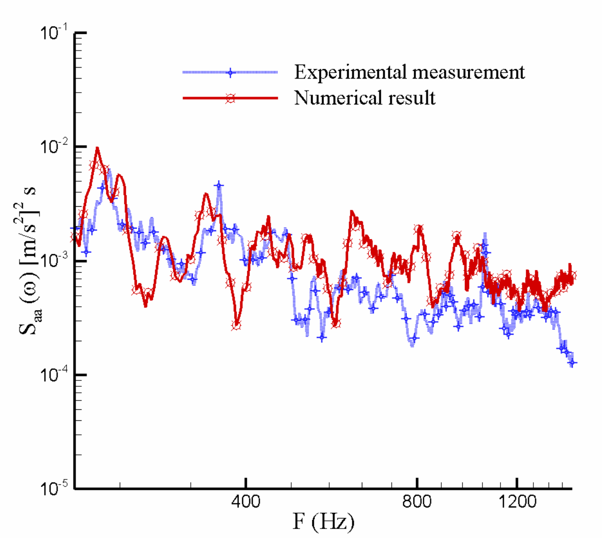

Figure 14 ASD of the shell acceleration: 5.45 m/s

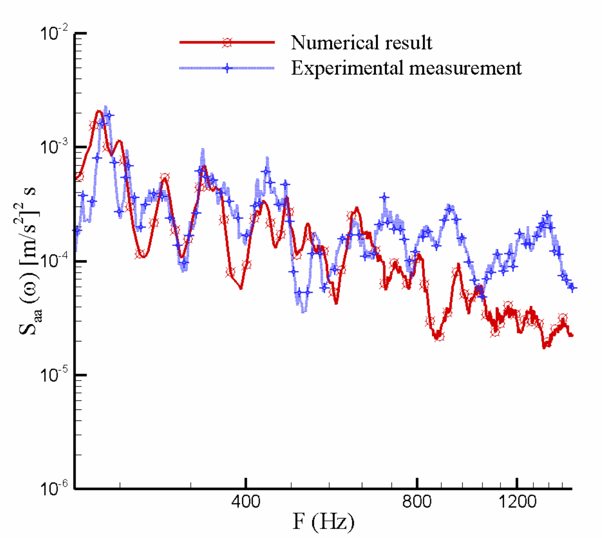

Figure 15 ASD of the shell acceleration: 3.64 m/s

On the contrary, analysing fig. 16 it is evident that classical model of wall pressure CSD do not provide a good representation of the load. In fact, the separation of the numerical and experimental response clearly highlights the inability of (1) to model the load. As already shown in Ref.3, transition is weakly non-homogeneous process that induces higher wall pressure fluctuations than those of a fully developed TBL at comparable Reynolds number. Thus, a different spatial model for its representation is needed. On the other side, pressure gradient effects can be taken into account in the CSD model by a lower convection velocity and a higher longitudinal decay coefficient.

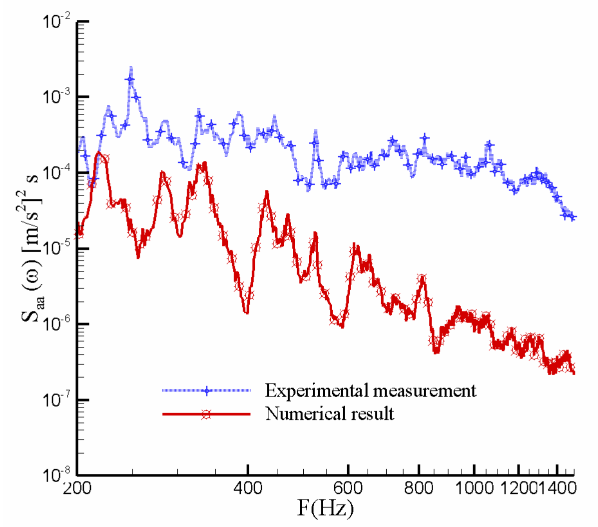

Figure 16 ASD of the shell acceleration: 2.72 m/s

CONCLUSIONS

In this paper the results of two experimental campaigns performed on a bulbous of a fast ship aimed at analyzing wall pressure fluctuations induced by turbulent boundary layer and the vibrations induced on an elastic section of the bulbous to this load have been presented.

From the analysis of both experimental and theoretical results it is possible to conclude that:

1) In presence of a mild APG and weak convex curvature classical scaling laws for pressure ASD do not provide a collapse of pressure fluctuations in all the frequency range. In fact, while high frequency spectra collapse well when normalized using inner flow variables, outer flow variables do not work.
2) With respect to previous measurements performed on flat plates, pressure spectra in presence of mild APG are characterized by higher amplitude in the low-mid frequency range. Notwithstanding a logarithmic region is still visible.
3) In late transition condition, ASD pressure spectra are characterized by a broad hump due to Tollmien-Schlichting waves. At initial transition condition, energy content is sensibly lower than for turbulent condition and highly oscillating.
4) Convection velocity is reduced by the presence of APG.
5) Streamwise decay factor increases when an APG acts along the flow, thus turbulent eddies decay faster than a ZPG flow.
6) Even in presence of a mild APG and curvature, Corcos model still manage to characterize the pressure load, as long as its parameter are suitable chosen to take into account the presence of pressure gradient.
7) Classical CSD models can be used to represent the spatial behavior of a late transitional boundary layer. In

the case of an initial transitional boundary layer a different CSD model is needed.

REFERENCES

1. Bull M.K., 1996. “Wall pressure fluctuations beneath turbulent boundary layers: some reflections on forty years of research”, Journal of Sound and Vibration, Vol. 190, 299-315.
2. Snarski S.R. and Lueptow R.M., 1995. “Wall pressure and coherent structures in a turbulent boundary layer on a cylinder in axial flow”, Journal of Fluid Mechanics, Vol. 286, 137-171.
3. Park S. and Lauchle G.C., 2009. “ Wall pressure fluctuation due to boundary-layer transition”, Journal of Sound and Vibration Vol. 319, 1067-1082.
4. Corcos, G.M., 1964. “The structure of turbulent pressure field in boundary-layer flows”. Journal of Fluid Mechanics, Vol. 18, 353-377.
5. Farabee T.M. and Casarella M.J.,1991. “Spectral features of wall pressure fluctuations beneath turbulent boundary layers”, Physics of Fluids A, Vol. 3, 2410-2420.
6. Ciappi, E., Magionesi, F., 2005. Characteristics of the turbulent boundary layer pressure spectra for high speed vessels. Journal of Fluids and Structures, Vol.21, 321-333.
7. Na, Y., Moin, P., 1996. “Direct numerical simulation of turbulent boundary layers with adverse pressure gradients and separation”. Report No. TF-68. Thermosciences Division Department of Mechanical Engineering, Stanford University.
8. Goody, M., 1999. “An experimental investigation of pressure fluctuations in three-dimensional turbulent boundary layers”. PHD Thesis, Department of Aerospace and Ocean Engineering, Virgiania Tech, USA.
9. Goody, M., 2004. “Empirical spectral model of surface pressure fluctuations”. AIAA Journal, Vol. 42(9), 1788-1794.
10. Schloemer H.H., 1966. “Effects of pressure gradients on turbulent boundary layer wall pressure fluctuations”, Journal of the Acoustical Society of America, Vol. 42(1), 93-113.
11. Gillis, J.C. and Johnston J.P., 1983. “Turbulent boundary-layer flow and structure on a convex wall and its redevelopment on a flat wall”. Journal of Fluid Mechanics, Vol. 135, 123-153.
12. Chase, D.M., 1980. “Modelling the wavevector-frequency spectrum of turbulent boundary layer wall pressure”. Journal of sound and Vibration, Vol. 70 (1), 29-67.
13. Efimtsov, B.M., 1982. “Characteristics of the field of turbulent wall pressure fluctuations at large Reynolds numbers”. Soviet Phisics-Acoustics, Vol. 28(4), 289-292.
14. Smol’yakov, A.V., Tkachenko, V.M., 1991. “Model of pseudonic turbulent wall pressures and experimental data”. Soviet Physics-Acoustic, Vol. 37(6), 627-631.
15. Ciappi E., Magionesi F., De Rosa S. and Franco F., 2009. “Hydrodynamic and hydroelastic analyses of a plate excited by the turbulent boundary layer”. Journal of Fluids and Structures, Vol. 25(2), 321-342.
16. Finnveden S., Birgersson F., Ross U., Kremer T., 2005. “A model for wall pressure correlation for prediction of turbulence-induced vibration”. Journal of Fluids and Structures, Vol. 20, 1127-1143.
17. Di Mascio, A., Broglia, R. and Favini, B., 2001. “A second order Godunov-type scheme for naval hydrodynamics”. In Godunov Methods: Theory and Applications. Kluwer Academic/Plenum Publishers, New York, 253-261.
18. Hong C., Shin K., Jeon J and Kim S., 2008. “Transitional wall pressure fluctuations on axisymmetric bodies”. Journal of the Acoustical Society of America, Vol. 124(5) 2767-2773
19. Bull, M.K., Thomas S.W., 1976. “High frequency wall pressure fluctuations in turbulent boundary layers”. Phisics of Fluids, Vol. 19, 597-599.
20. Gravante, S.P., Naguib, A.M., Wark, C.E. and Nagib, H.M., 1998. “ Characterization of the pressure fluctuations under a fully developed turbulent boundary layer”. AIAA Journal, Vol. 36, 1811-1816.
21. Neves J.C., Moin P. and Moser R.D., 1994. “Effects of convex Transverse curvature on Wall-Bounded Turbulence. Part I. The velocity and vorticity”. Journal of Fluid Mechanics, Vol. 272, 349-381.
22. Willmarth, W.W. and Wooldridge, C.E., 1962. “Measurements of the fluctuating pressure at the wall beneath a thick turbulent boundary layer”. Journal of Fluid Mechanics, Vol. 14, 187-210.
23. .Elishakoff I., 1983. Probabilistic Methods in the Theory of Structures. John Wiley & Sons, ISBN 0471875724
24. De Rosa S., Pezzullo, G.,Lecce, L., Marulo, F., 1994. Structural Acoustic Calculations in the Low Frequency Range. AIAA Journal of Aircraft, Vol. 31(6), 1387-1394.